Structural, magnetic and electrical properties of the sol-gel prepared $Li_{0.5}Fe_{2.5}O_4$ fine particles

2006 J. Phys. D: Appl. Phys. 39 900

(http://iopscience.iop.org/0022-3727/39/5/002)

INSTITUTE OF PHYSICS PUBLISHING JOURNAL OF PHYSICS D: APPLIED PHYSICS

J. Phys. D: Appl. Phys. **39** (2006) 900–910 doi:10.1088/0022-3727/39/5/002

Structural, magnetic and electrical properties of the sol-gel prepared $Li_{0.5}Fe_{2.5}O_4$ fine particles

Mathew George[1], **Swapna S Nair**[1], **Asha Mary John**[1], **P A Joy**[2], **M R Anantharaman**[1,3]

[1]Department of Physics, Cochin University of Science and Technology, Cochin-682 022, India

[2] Physical Chemistry Division, National Chemical Laboratory, Pune-411 008, India

E-mail: mra@cusat.ac.in

Received 20 May 2005, in final form 23 December 2005
Published 17 February 2006
Online at stacks.iop.org/JPhysD/39/900

Abstract

Fine particles of lithium ferrite were synthesized by the sol-gel method. By subsequent heat treatment at different temperatures, lithium ferrites of different grain sizes were prepared. A structural characterization of all the samples was conducted by the x-ray diffraction technique. A grain size of around 12 nm was observed for $Li_{0.5}Fe_{2.5}O_4$ obtained through the sol-gel method. Magnetic properties of lithium ferrite nanoparticles with grain size ranging from 12 to 32 nm were studied. Magnetization measurements showed that $Li_{0.5}Fe_{2.5}O_4$ fine particles exhibit a deviation from the predicted magnetic behaviour. The as-prepared sample of lithium ferrite showed a maximum saturation magnetization of 75 emu g^{-1}. Variation of coercivity is attributed to the transition from multi-domain to single domain nature. Dielectric permittivity and ac conductivity of all the samples were evaluated as a function of frequency, temperature and grain size. Variation of permittivity and ac conductivity with frequency reveals that the dispersion is due to the Maxwell–Wagner type interfacial polarization.

1. Introduction

Magnetic nanoparticles continue to be a fascinating subject of interest both from the fundamental and application point of view [1]. Their properties at the nanolevel are quite different from their coarser sized cousins and they exhibit altogether different magnetic and electrical properties [2–6].

Lithium ferrites ($Li_{0.5}Fe_{2.5}O_4$) are useful materials for microwave devices and memory core applications [7–10]. Lithium ferrite crystallizes in the inverse spinel structure. Though lithium ferrites have been a thoroughly investigated ferrite system [10, 11], because of their excellent square sloop characteristics, this system is being revisited to investigate the finite size effects as well as to devise new materials based on lithium ferrite for microwave and other applications. Synthesis of structurally stabilized lithium ferrite with and without flux is still a hot topic of research in the area of magnetic materials.

Magnetic saturation, coercivity, magnetization and loss change drastically as the size of the particles move down to the nanometric range [12–17]. As the grain size of $Li_{0.5}Fe_{2.5}O_4$ decreases the coercivity increases, reaches a maximum and then decreases. This change in coercivity is attributed to the transition from a multidomain to a single domain structure. Reduction in saturation magnetization has been observed in magnetic nanoparticles, especially in ferrites and has been related, alternatively, to surface anisotropy, surface spin disorder or finite size effects. However fine particles of $Li_{0.5}Fe_{2.5}O_4$ show a deviation from the theoretically predicted value of magnetization.

Lithium ferrite is a high resistive semiconductor having low eddy-current losses [18, 19]. The electrical properties of ferrites are dependent upon several factors, namely, method of preparation, grain size, chemical composition, sintering temperature and atmosphere [20, 22]. The wider use of lithium ferrites particularly in microwave devices is restricted

[3] Author to whom any correspondence should be addressed.

due to the difficulties experienced in sintering the material at the high temperatures employed to achieve high densities in stoichiometric form. The irreversible loss of lithium and oxygen during sintering was the main cause that made lithium ferrites technologically difficult to prepare. The sol-gel method provides an easy alternative for the preparation of nano $Li_{0.5}Fe_{2.5}O_4$ at low temperatures. Lithium ferrite was prepared by the sol-gel method and was heat treated to change the particle dimensions. The magnetic and electrical properties have been studied with a view to correlating the properties. The details of the findings are reported here.

2. Experimental techniques

2.1. Synthesis techniques

Fine particles of $Li_{0.5}Fe_{2.5}O_4$ have been prepared by the sol-gel technique. Analytical grades of $Fe(NO_3)_3 \cdot 9H_2O$ and $LiNO_3.3H_2O$ were dissolved in ethylene glycol in the ratio 2.5 : 0.5 at about 40 °C. After heating the sol of the metal compounds to around 60 °C a wet gel is obtained. The obtained gel when dried at about 80 °C self-ignites to give a highly voluminous and fluffy product of $Li_{0.5}Fe_{2.5}O_4$. $Li_{0.5}Fe_{2.5}O_4$ with varying grain sizes were obtained by heat treating different portions of the as-prepared powder separately for 12 h at 300, 600 and 900 °C.

2.2. X ray diffraction studies

The structural characterization of all the four samples was carried out by the x-ray diffraction (XRD) technique on a Rigaku D_{max}/2C diffractometer with a nickel filter using Cu-K_α radiation (wavelength $\lambda = 1.5418$ Å).

The average grain size was determined from the measured width of their diffraction curves using the Debye Scherrer formula

$$D = \frac{0.9\lambda}{\beta \cos\theta} \tag{1}$$

Here λ is the wavelength of the Cu K_α radiation ($\lambda = 1.5418$ Å), β is the integral width in radians. Debye Scherrer's formula assumes approximations and gives the average grain size if the grain size distribution is narrow and strain induced effects are quite negligible. The contribution due to instrumental broadening has to be taken into account in order to obtain the accurate grain size.

The x-ray density of the prepared ceramic samples was calculated using the relation

$$\rho_x = \frac{nM}{a^3 N}, \tag{2}$$

where n is the number of molecules/unit cell, M is the molecular weight, a is the lattice parameter and N is the Avogadro number. The apparent density is calculated by considering the cylindrical shape of the pellets and using the relation

$$\rho_a = \frac{m}{V} = \frac{m}{\pi r^2 h}, \tag{3}$$

where m is the mass, r the radius and h the thickness of the pellet. Porosity P of the ferrite samples was then determined by employing the relation

$$P = \frac{\rho_x - \rho_a}{\rho_x}. \tag{4}$$

The surface area in metresquare per kilograms was obtained using the relation

$$S = \frac{6}{D\rho_a}, \tag{5}$$

where 'D' is the diameter of the particle in nanometres and 'ρ_a' the density of the particle in kilograms per metrecube. (If the diameter is measured in nanometres and density in grams per centimetre cube, S becomes $6000/D\rho_a$).

2.3. Magnetic measurements

Magnetic measurements were carried out using a vibrating sample magnetometer (EG & G PAR 4500) for all the four samples at room temperature. The magnetic properties such as saturation, magnetization and coercivity were elucidated from the hysteresis curve.

2.4. Electrical characterization

The electrical properties of lithium ferrite samples were carried out using a homemade cell and an LCR meter HP 4285A. Pellet-shaped samples were employed for the evaluation of the electrical properties. The data acquisition was completely automated using a virtual instrumentation package called LabVIEW, a propriety of National Instruments. The dielectric permittivity (ε_r) of the samples was calculated using the relation

$$\varepsilon_r = \frac{Cd}{\varepsilon_0 A}, \tag{6}$$

assuming 100% filling factor, where 'C' is the measured value of capacitance of the sample, 'd' is the thickness, 'A' is the surface area, and 'ε_0' is the dielectric permittivity of air. From the dielectric loss and dielectric permittivity, ac conductivity of ferrite samples can be evaluated using the relation

$$\sigma_{ac} = 2\pi\varepsilon_0\varepsilon_r f \tan\delta, \tag{7}$$

where, f is the frequency of the applied field, ε_0 is the absolute permittivity of air, ε_r is the relative permittivity of the samples, $\tan\delta$ is the loss factor and σ_{ac} is temperature and frequency dependent [22], and it is attributed to the dielectric relaxation caused by localized electric charge carriers which obey the power law [23].

$$\sigma_{ac}(\omega, T) = B\omega^n, \tag{8}$$

where B and n are the composition and temperature dependent parameters.

3. Results and discussions

Figure 1 shows the x-ray diffractograms of lithium ferrites sintered at various temperatures. As the sintering temperature increases the width of the central maxima decreases and the intensity of the peaks increases. This is due to the increase in the grain size of the ferrite particles as the firing temperature increases. The grain sizes of the samples were evaluated by measuring the FWHM. The results are shown in table 1.

Figure 2(*a*) represents the variation of grain size with firing temperature. From the graph it can be noticed that grain size increases upon firing. The change is more prominent at a high

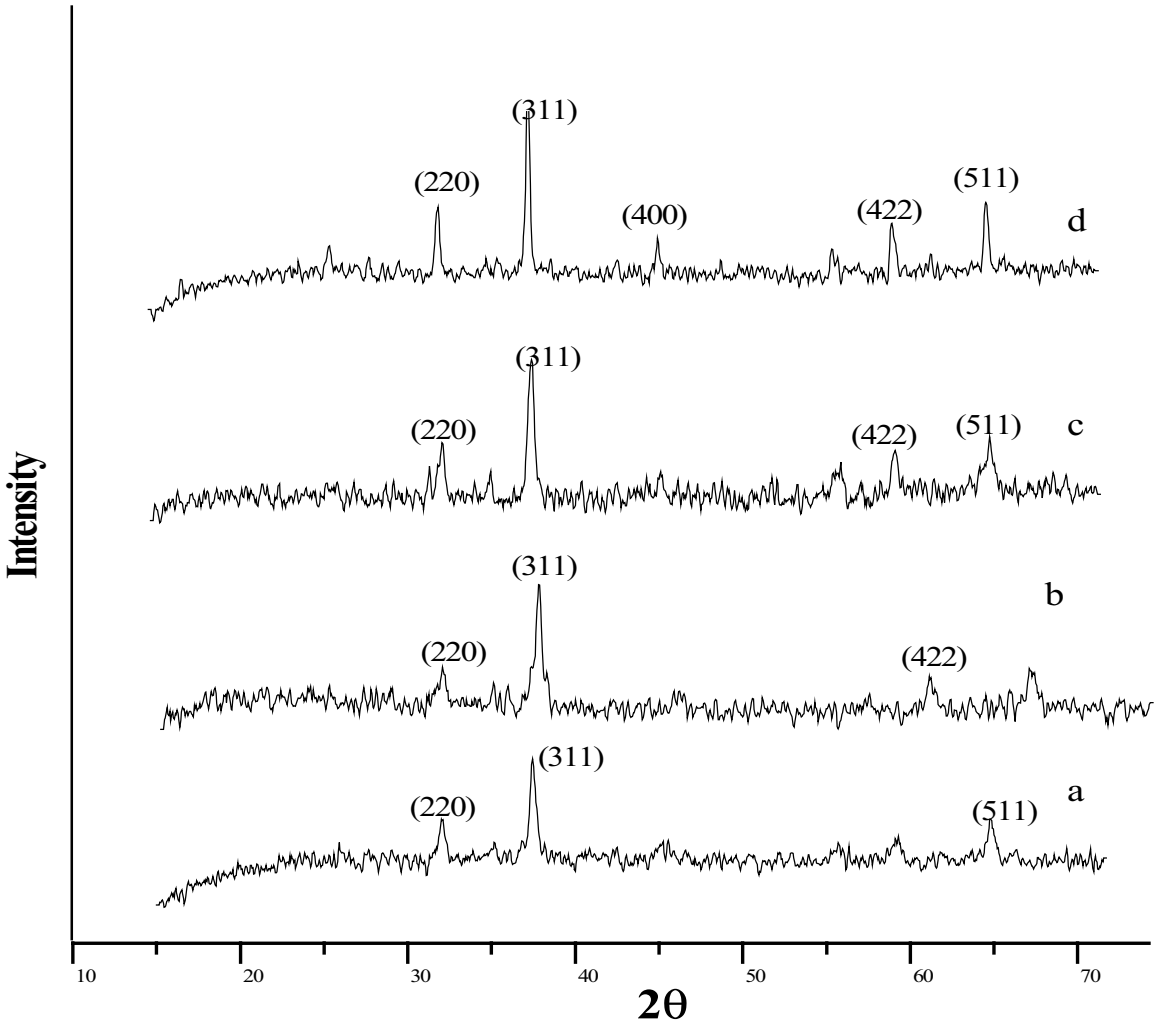

Figure 1. X-ray diffraction patterns of the (*a*) as-prepared $Li_{0.5}Fe_{2.5}O_4$ powder, (*b*) the $Li_{0.5}Fe_{2.5}O_4$ powder heated at 300 °C, (*c*) at 600 °C and (*d*) 900 °C.

Table 1. Structural parameters of the sol-gel synthesized $Li_{0.5}Fe_{2.5}O_4$.

Firing temperature (°C)	Grain size (nm)	Specific surface area ($m^2\ g^{-1}$)	Theoretical density ($g\ cc^{-1}$)	Experimental density ($g\ cc^{-1}$)	Porosity (%)
As-prepared powder	12	109	4.68	3.1	34
300	14	90	4.70	3.8	19
600	22	59	4.73	4.2	11
900	32	39	4.74	4.4	6.5

temperature. The specific surface area of the particles increases as the grain size decreases. The variation pattern is shown in figure 2(*b*).

The variation of the porosity of the samples with firing temperature is shown in figure 3. The as-prepared sol-gel samples are 34% porous and the samples sintered at 900 °C exhibited a porosity of ∼6.5%. This indicates that high temperature sintering is necessary to achieve maximum density for lithium ferrite.

3.1. Magnetic properties of lithium ferrites

Figure 4 shows the hysteresis curve for the $Li_{0.5}Fe_{2.5}O_4$ particles measured at room temperature. Parameters such as saturation magnetization and coercivity were determined from the hysteresis graph.

The as-prepared sample of lithium ferrite shows a maximum saturation magnetization of 75 emu g^{-1} which is quite large a value as compared with the value predicted by Neel's two sub lattice model. This deviation is quite anomalous considering the fact that $Li_{0.5}Fe_{2.5}O_4$ in the bulk are known to obey Neel's two sub lattice model. The deviation displayed in the saturation magnetization of these materials may arise from a multitude of factors. Among them surface effects/surface spins/cation redistribution are the prominent ones. It may be noted that ultra fine nickel ferrites and zinc ferrites exhibited an increase in magnetization with respect

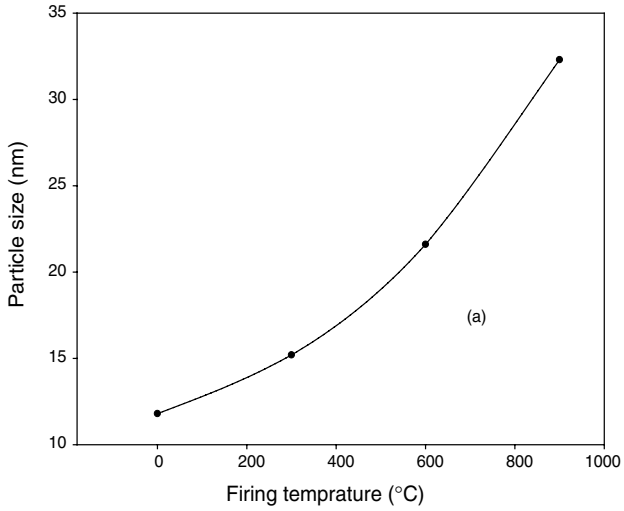

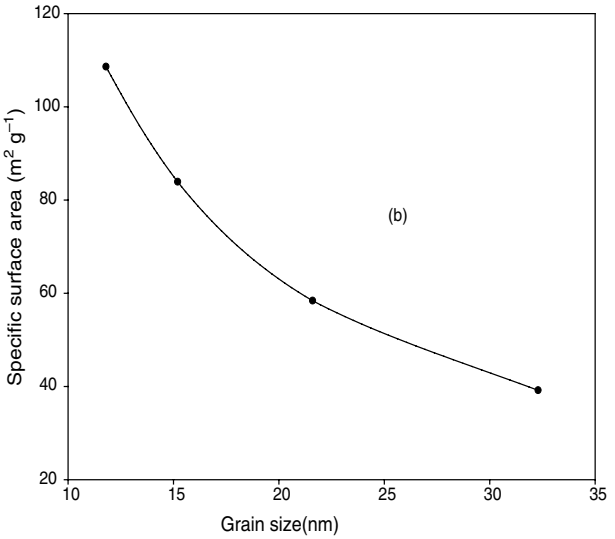

Figure 2. Variation of (*a*) grain size with firing temperature and (*b*) Specific surface area with grain size.

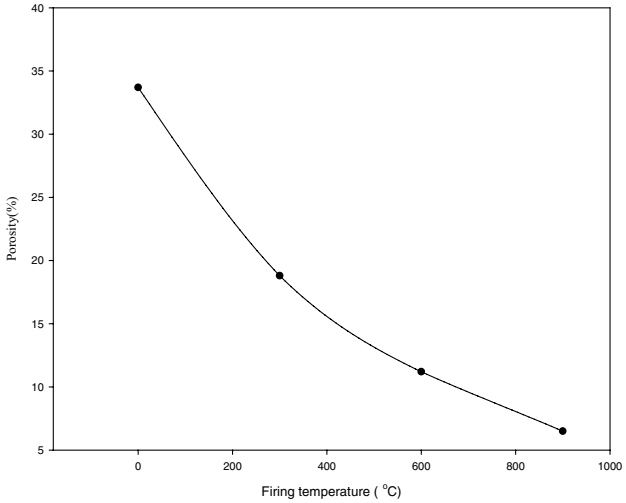

Figure 3. Variation of porosity with firing temperature for $Li_{0.5}Fe_{2.5}O_4$.

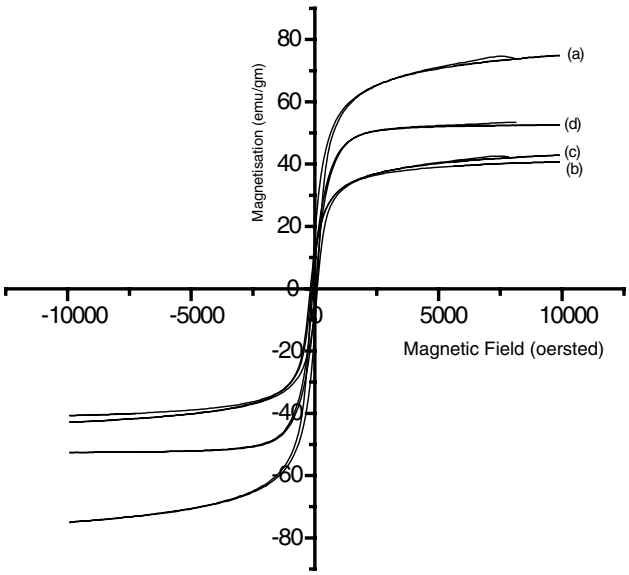

Figure 4. Hysteresis curve for the sol-gel synthesized (*a*) as-prepared $Li_{0.5}Fe_{2.5}O_4$ powder, (*b*) $Li_{0.5}Fe_{2.5}O_4$ powder heat treated at 300 °C, (*c*) 600 °C and (*d*) 900 °C.

to their counterparts in the micron regime [24–26]. Various researchers have reported this anomaly and have invoked different hypotheses and theories to explain the observed modification of magnetic properties in the ultra fine regime. In ultra fine particles, the surface-to-volume ratio becomes large in such a way that the contribution from the surface determines the bulk properties. For example Anantharaman *et al* and Shenoy *et al* [24,25] have reported that ultra fine zinc ferrite becomes magnetic due to pronounced surface effects such as the occurrence of surface spins contributing to the total magnetization. Chinnasamy *et al* [26] have attributed the increase in magnetization to the redistribution of cations in the lattice when particles are in the nanoregime. It is reported that due to cation redistribution ultra fine nickel ferrites show an 8% increase in the value of M_s compared with the theoretically predicted value [26]. Such a possibility could not be ruled out in the case of ultrafine lithium ferrite. However this requires a thorough study employing Mossbauer spectroscopy.

Figure 5 shows the variation of magnetization with grain size. However the variation of magnetization parameters with firing temperature is not entirely due to the variation in grain size. In the ultra fine regime the anomalous enhancement in saturation magnetization is due to the fine particle grains. But the decrease in magnetization values thereafter could be attributed to several other phenomena.

The magnetization of the sample sintered at 300 °C drops to 42.8 emu g^{-1} and the sample sintered at 600 °C has a saturation magnetization of 40.8 emu g^{-1}. Further firing at 900 °C increases the magnetization. This is due to the volatization of lithium and oxygen .The loss of Li_2O results in the formation of α-Fe_2O_3, thereby reducing the saturation magnetization. From the XRD, it can be seen that the peak corresponding to haematite increased for the sample fired at 300 °C and the increase becomes conspicuous for the sample fired at 600 °C. On further firing α-Fe_2O_3 is present only in traces. This confirms the volatization of $Li_{0.5}Fe_{2.5}O_4$ and the formation of α-Fe_2O_3. The presence of haematite which is

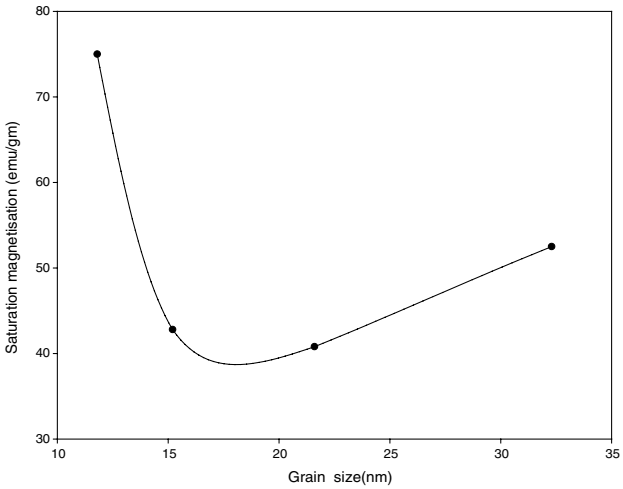

Figure 5. Variation of saturation magnetization with the grain size of $Li_{0.5}Fe_{2.5}O_4$.

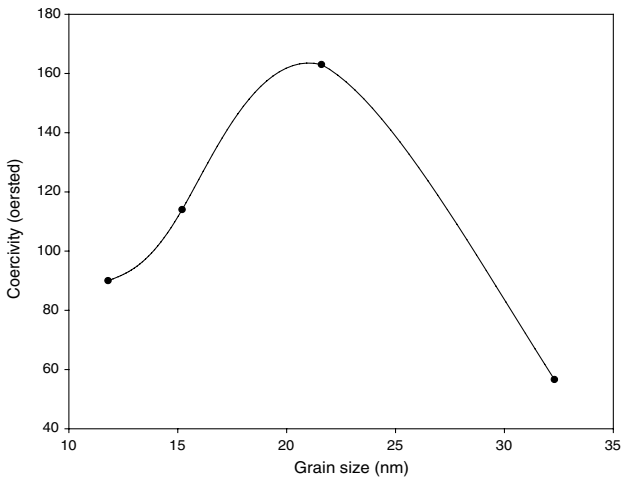

Figure 6. Variation of coercivity with the grain size of $Li_{0.5}Fe_{2.5}O_4$.

antiferromagnetic in nature reduces the value of saturation magnetization considerably.

Figure 6 shows the variation of coercivity with the average grain size of the lithium ferrite at room temperature. It is evident from the graph that as the grain size increases, the value of coercivity increases, reaches a maximum and then decreases. This variation of H_c with grain size can be explained based on the domain structure, critical particle diameter and the anisotropy of the material.

The coercivity of magnetic samples has a striking dependence on their size. As the grain size decreases, the coercivity increases reaches a maximum and then decreases. The change in coercivity is attributed to its change from the multidomain nature to the single domain. In the multidomain region the variation of coercivity with grain size is expressed as [12],

$$H_c = a + \frac{b}{D}, \tag{9}$$

where 'a' and 'b' are constants and 'D' is the diameter of the particle. Hence in the multidomain region the coercivity decreases as the particle diameter increases. Below the critical diameter D_s, the coercivity decreases because of thermal effects. As the grain size decreases H_c decreases below a critical grain size as governed by the equation.

$$H_{ci} = g - \frac{h}{D^{3/2}}, \tag{10}$$

where 'g' and 'h' are constants. A material will spontaneously break up into a number of domains in order to reduce the large magnetization energy if it is a single domain. The ratio of the energies before and after division into domains varied as $\sqrt{D}$, where D is the particle diameter. Thus as D becomes smaller, the reduction in energy becomes smaller and this suggests that for very small D the material prefers to remain in the single domain.

3.2. Electrical properties of lithium ferrites

3.2.1. Frequency dependence of electrical properties.

Dielectric permittivity. The frequency dependence of the dielectric permittivity for all the samples was studied at various temperatures. Figure 7(*a*)–(*d*) depicts the variation of permittivity with frequency. Dielectric permittivity decreases as frequency increases from 100 KHz to 8 MHz. The decrease is rapid at lower frequencies and slower at higher frequencies. Similar results were observed for other systems of ferrites [27–29]. The decrease in permittivity with frequency can be explained on the basis of Koops theory [30], which considers the dielectric structure as an inhomogeneous medium of two layers of the Maxwell–Wagner type [31].

In this model, the dielectric structure is assumed to be consisting of well-conducting grains which are separated by poorly conducting grain boundaries. It was found that for ferrites, the permittivity is directly proportional to the square root of conductivity [28]. Therefore the grains have higher values of conductivity and permittivity, while the grain boundaries have lower values. At lower frequencies the grain boundaries are more effective than grains in electrical conduction. Therefore permittivity is high at lower frequencies and decreases as frequency increases. The decrease in permittivity takes place when the jumping frequency of electric charge carriers cannot follow the alternation of the applied ac electric field beyond a certain critical frequency.

A theoretical fit for the Maxwell–Wagner theory of dielectric dispersion is provided in figure 7(*e*). The fit for experimental data is not in complete agreement and this deviation may be because of the fact that it is assumed that the filling factor is 100%. However it may be noted that the variation pattern of permittivity with frequency is almost in accordance with the theory. Also in nanograins, there is a contribution from the high surface area which may affect the frequency variation.

ac conductivity. Figure 8(*a*)–(*d*) represents the variation of ac conductivity with logarithmic frequency in the frequency range of 100 KHz–8 MHz. The ac conductivity shows an increasing trend with the increase in frequency for all the samples. Its value first increases linearly according to the power law (equation (8)). A theoretical fit for a representative sample is provided figure 8(*e*) in which the logarithmic ac conductivity variation is linear in frequency in the low frequency regime

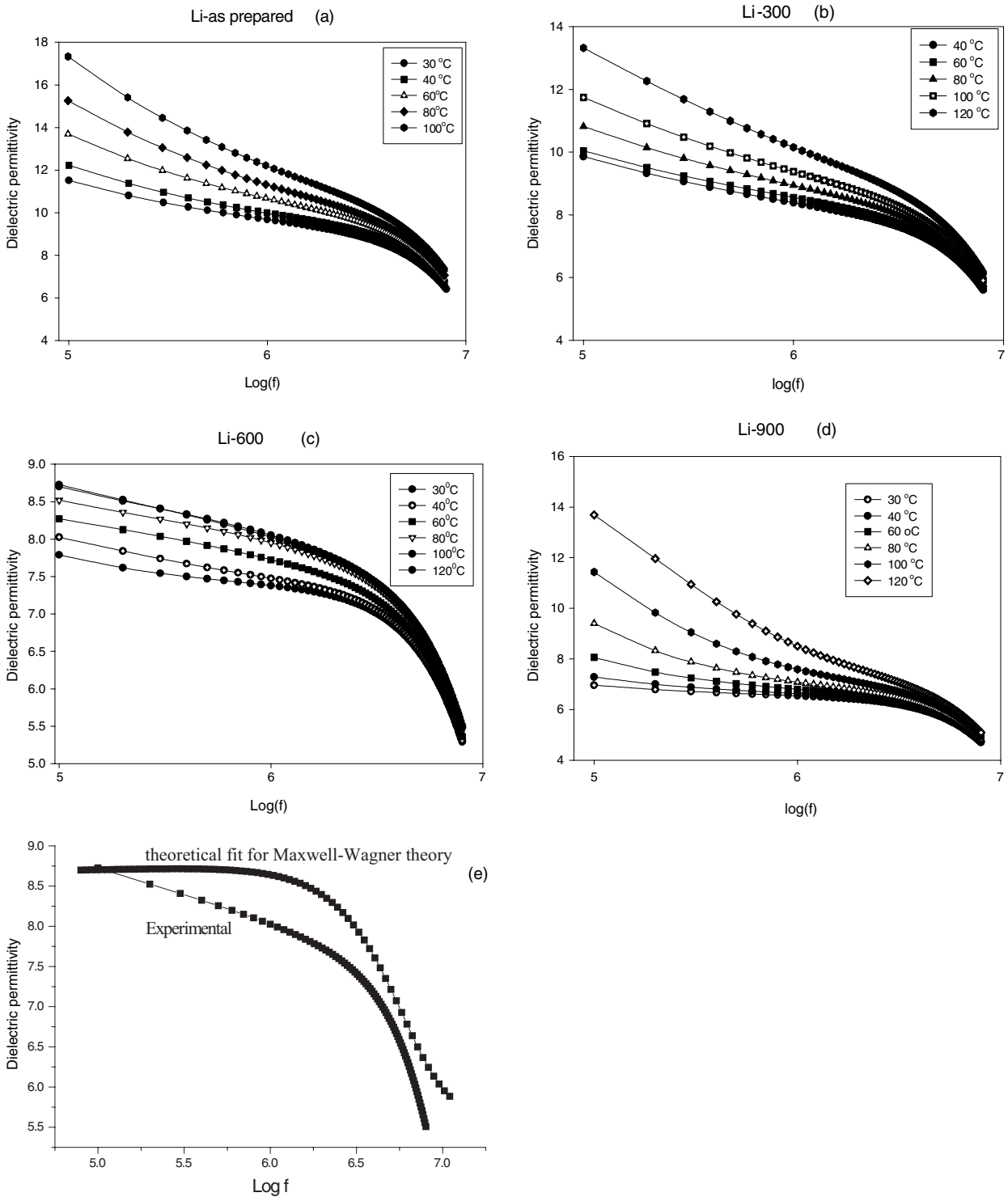

Figure 7. Variation of dielectric permittivity with logarithmic frequency for the sol-gel synthesized as-prepared $Li_{0.5}Fe_{2.5}O_4$ powder (*a*), and the $Li_{0.5}Fe_{2.5}O_4$ powder heat treated at 300 °C (*b*), 600 °C (*c*) and 900 °C (*d*). Theoretical fit (*e*) for Maxwell–Wagner theory of dielectric dispersion (Li 600-RT).

whose slope gives the value of '*n*' in the power law. The value of '*n*' is close to unity for almost all the samples studied. The value of conductivity at zero frequency also could be deduced from this which is of the order of 10^{-9} S cm^{-1}. But at higher frequencies the ac conductivity decreases.

This behaviour is akin to the Maxwell–Wagner type. The dielectric structure of ferrites is given by Koops Phenomenological theory and Maxwell–Wagner theory [30, 31]. At lower frequencies the grain boundaries are more active and hence the hopping of Fe^{2+} and Fe^{3+} ion is less at lower frequencies. As the frequency of the applied field increases, the conductive grains become more active thereby promoting the hopping between Fe^{2+} and Fe^{3+} ions, thereby increasing the hopping conduction. A gradual increase in

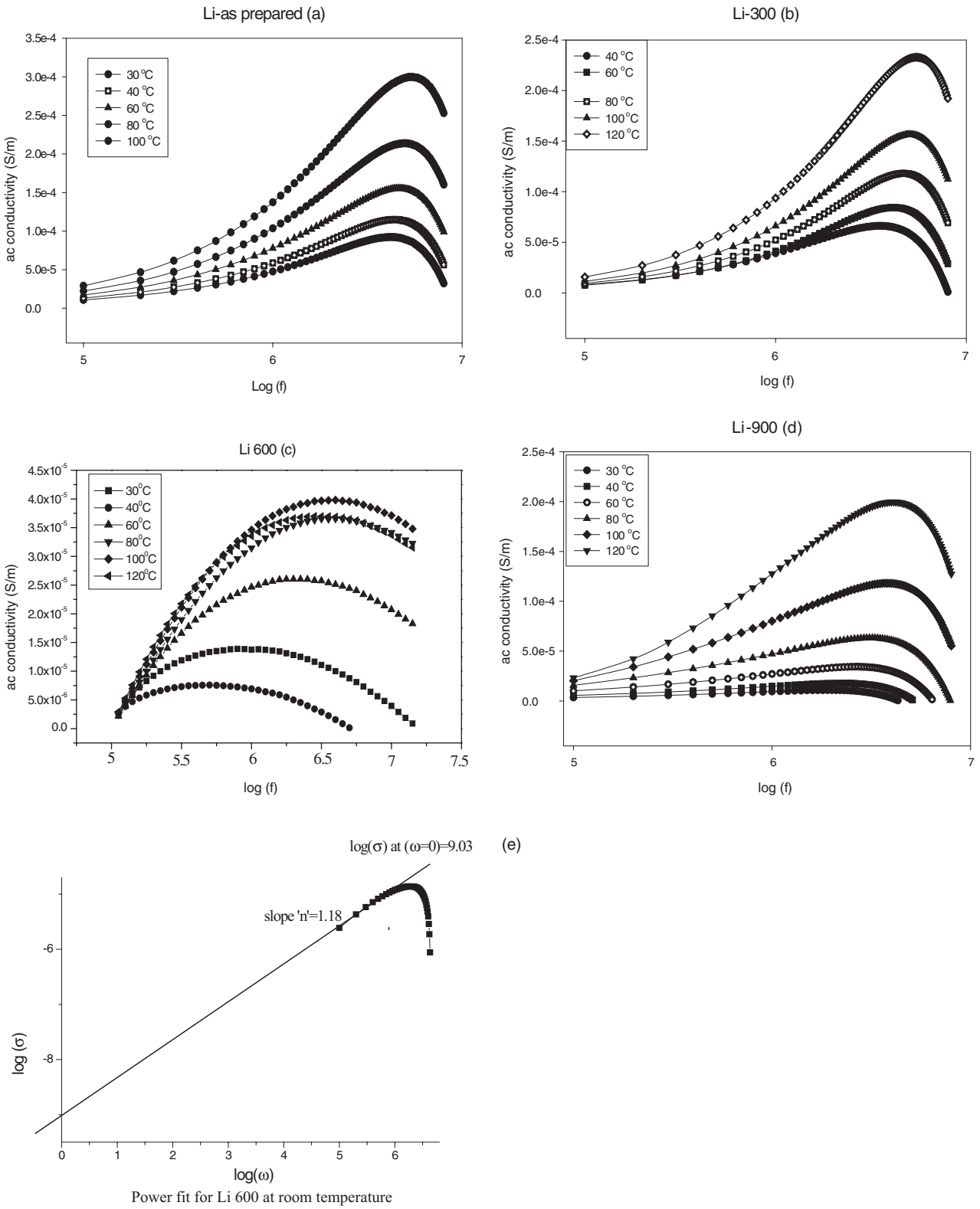

Figure 8. Variation of ac conductivity with logarithmic frequency for the sol-gel synthesized as-prepared $Li_{0.5}Fe_{2.5}O_4$ powder (*a*) and the $Li_{0.5}Fe_{2.5}O_4$ powder heat treated at 300 °C (*b*), 600 °C (*c*), and 900 °C (*d*). Theoretical fit (*e*) for the power law for a representative sample (for the determination of '*n*' and σ_{ac} at $\omega = 0$).

conductivity was observed with frequency. But at higher frequencies the frequency of the hopping ions could not follow the applied field frequency and it lags behind. This causes a decrease in conductivity at higher frequencies. According to the power law the logarithmic relation between the ac conductivity and the angular frequency represents straight lines with slopes equal to the exponent n and the intercept equal to $\log \omega$ on the vertical axis at $\log \omega = 0$. Various

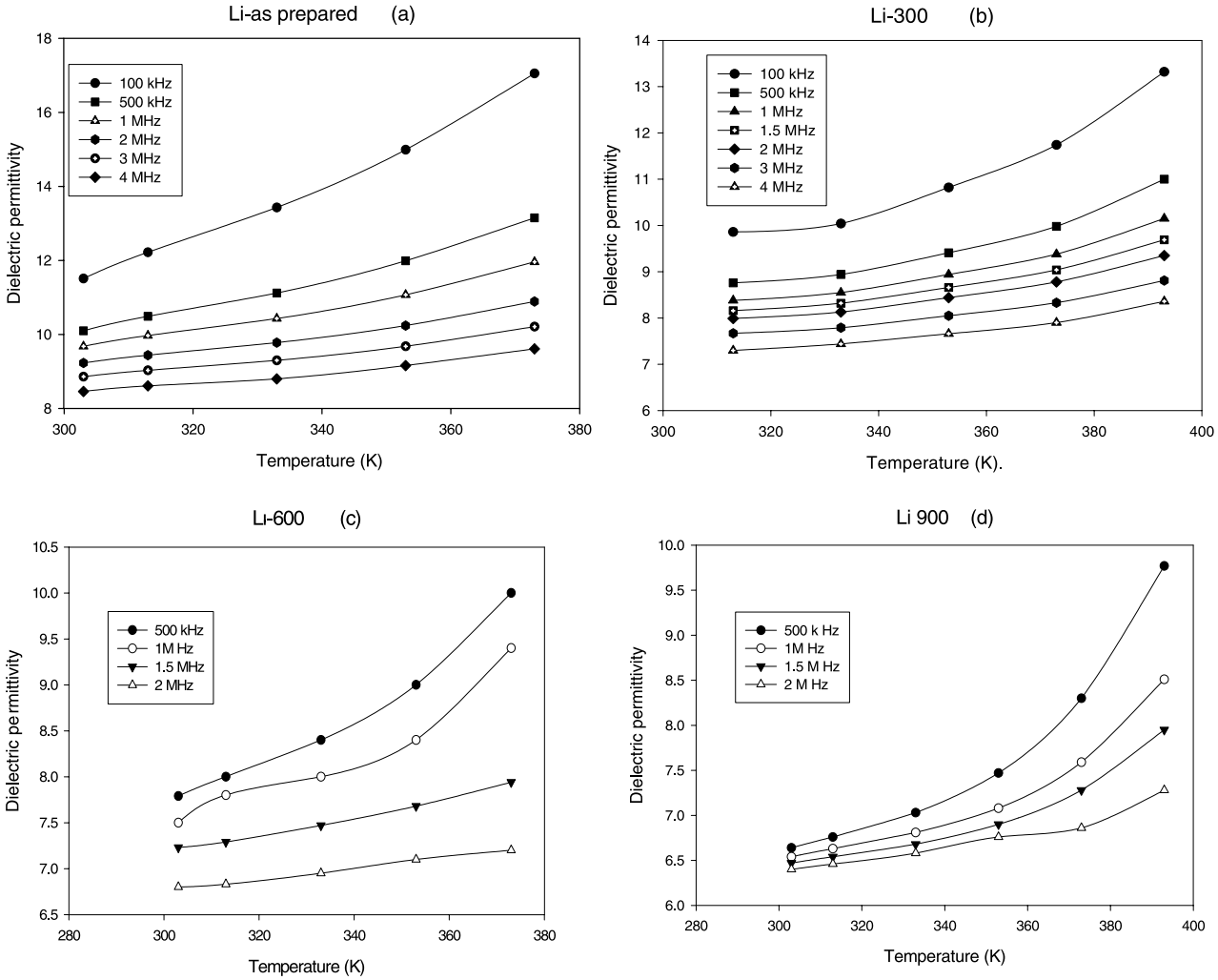

Figure 9. Temperature dependence of dielectric permittivity for the sol-gel synthesized as-prepared $Li_{0.5}Fe_{2.5}O_4$ powder (*a*), and the $Li_{0.5}Fe_{2.5}O_4$ powder heat treated at 300 °C (*b*), 600 °C (*c*) and 900 °C (*d*).

researchers [22, 23] have found that at temperature $> T_c$ the conductivity is dependent on frequency. Here it must be noted that the temperatures employed for studying the variation are much below T_c.

3.2.2. Temperature dependence of electrical properties.

Dielectric permittivity. Figure 9 shows the variation of permittivity with temperature. It is observed that the dielectric permittivity increases slowly with temperature in the low temperature region up to 373 K and above this temperature, permittivity increases rapidly for all samples.

The resistivity of ferrites decreases with the increase in temperature because ferrites were considered magnetic semiconductors. According to Koops, the dielectric permittivity is inversely proportional to the square root of resistivity. Therefore an increase in dielectric permittivity with temperature is expected. The high dielectric permittivity at low frequencies and high temperature is due to the presence of permanent dipole moments indicating a small effective charge separation [27, 28]. This small separation must be due to the asymmetric fields experienced by either oxygen or metallic ions. In most cases, the atoms or molecules in the samples cannot orient themselves at a low temperature region. When temperature rises, the orientation of these dipoles is facilitated and this increases the dielectric polarization. At very high temperatures the chaotic thermal oscillations of molecules are intensified and the permittivity passes through a maximum value.

At lower frequencies, an equation of the form $\varepsilon = \varepsilon_0 + A\exp(BT)$ can be fitted where ε and ε_0 are the dielectric permittivity at temperature T and 0 K, respectively, and A and B are constants. This relation holds good only at lower frequencies. For higher frequencies, variation in ε is nominal since the dipoles are not free to orient at a higher frequency and hence the orientation polarization will be less at higher frequencies. Thus the total increase in polarization will be less with the rise in temperature at higher frequencies. This explains the change in the dielectric constant with temperature at higher frequencies.

ac conductivity. The variation of ac conductivity with temperature of $Li_{0.5}Fe_{2.5}O_4$ samples is shown in figure 10. It was observed that at higher temperatures the conductivity is higher and as the temperature decreases the conductivity also decreases, but a marked difference is found in this

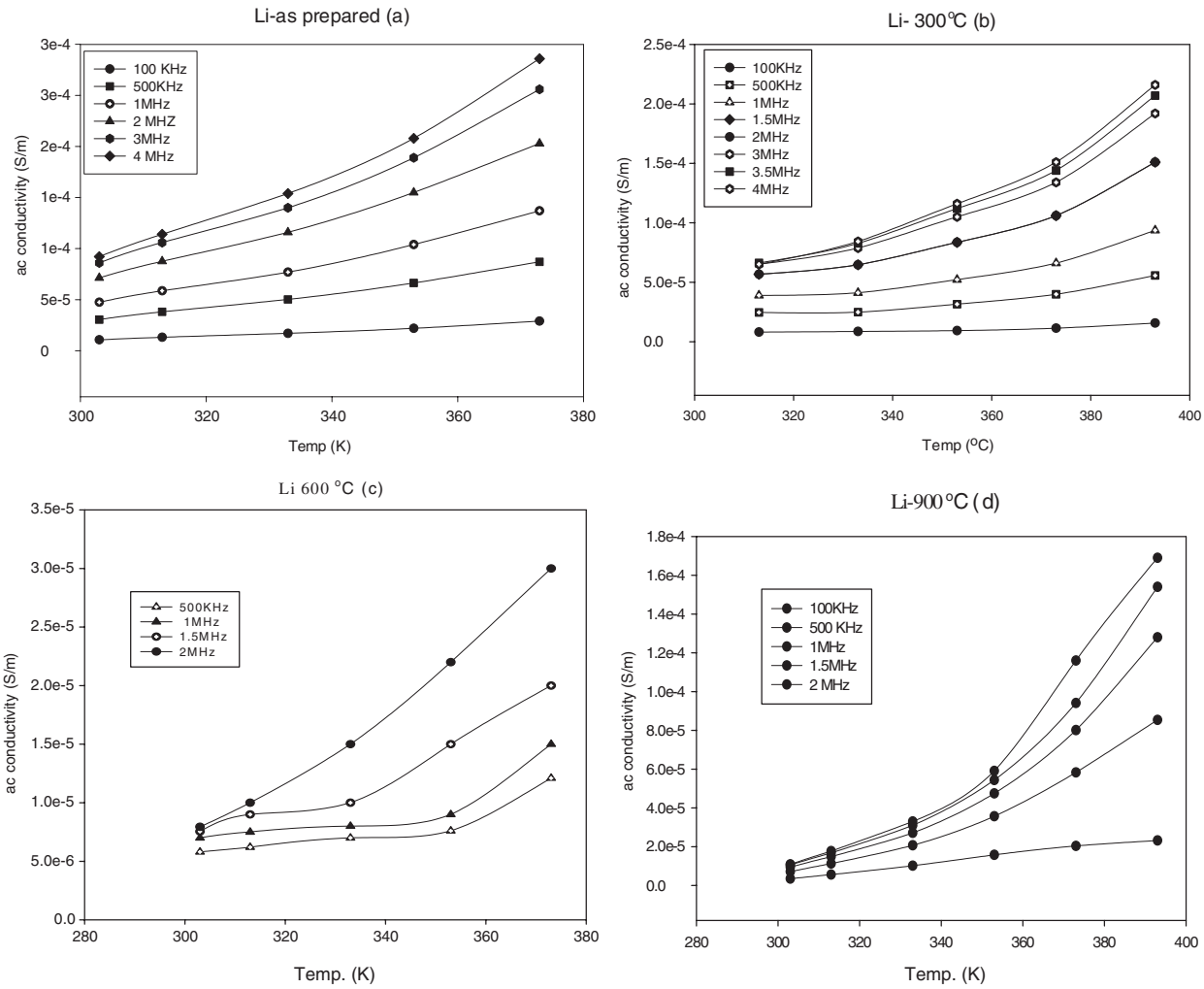

Figure 10. Variation of ac conductivity with temperature for the sol-gel synthesized as-prepared $Li_{0.5}Fe_{2.5}O_4$ powder (*a*), and the $Li_{0.5}Fe_{2.5}O_4$ powder heat treated at 300 °C (*b*), 600 °C (*c*) and 900 °C (*d*).

variation at low and high frequencies. At low frequencies the ac conductivity increases with increase in temperature while at higher frequencies the conductivity increases sharply to a certain temperature and thereafter the rate of change of conductivity increases significantly with the increase in temperature. The conductivity increases with the increase in frequency at all temperatures, but at lower temperatures this difference is not very prominent. The increase in the electrical conductivity with the increase in temperature is attributed to the increase in drift mobility of the thermally activated charge carriers according to the hopping conduction mechanism. Increasing temperature thermally activates the electron exchange between Fe^{2+} and Fe^{3+} ions on the octahedral sites. This electron exchange causes local displacements in the direction of the applied electric field; this includes the dielectric polarization in ferrites.

As temperature increases, ac conductivity increases due to the increase in drift mobility of the thermally activated electrons [20,21]. Also the space charge polarization is caused by the number of space charge carriers. With the rise in temperature the number of carriers increases resulting in an enhanced build-up of space charge polarization and hence an increase in the conductivity. Above the Curie temperature the term n in the power law becomes equal to zero because the power law becomes invalid and the conductivity is frequency independent and is equal to dc conductivity. Therefore, n decreases as temperature increases. So the electrical conduction becomes frequency dependent for $0 < n < 1$.

3.2.3. Grain size dependence of electrical properties. The grain size, grain boundaries, porosity and sintering temperature are important factors influencing the conductivity and permittivity. Both dielectric permittivity and ac conductivity are found to decrease as the grain size of the ferrite particles increase (figure 11). The comparatively lower value of resistivity or the higher value of permittivity in samples sintered at lower temperatures are possibly due to the presence of a localized state in the forbidden energy gap which arises due to lattice imperfections. The presence of these states effectively lowers the energy barriers to the flow of electrons.

According to the correlated barrier hopping model [32,33] ac conductivity

$$\sigma(\omega) = \frac{\pi^3}{24} N^2 \varepsilon R_\omega^6 \omega, \tag{11}$$

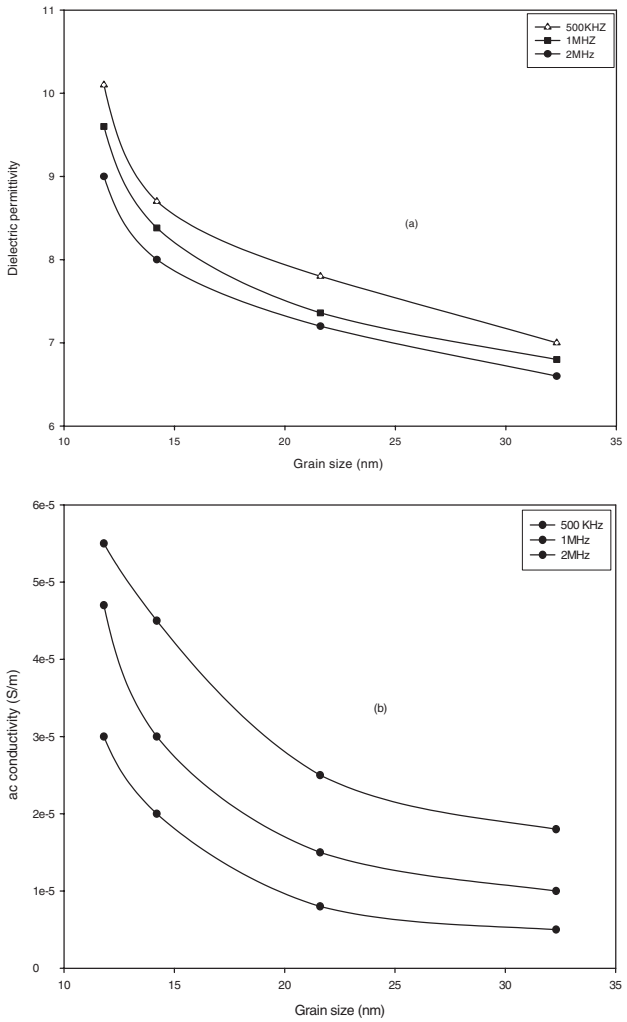

Figure 11. Grain size dependence of (*a*) dielectric permittivity (*b*) ac conductivity.

where, N is the concentration of defect sites contributing to the hopping mechanism, ε, the dielectric permittivity and R_ω, the hopping distance. Increasing the sintering temperature results in more uniform crystal structures with reduced imperfections thereby decreasing the value of N, which ultimately reduces the value of ac conductivity. Hence samples fired at high temperature or samples with greater grain size possess a low value of conductivity. A similar trend in conductivity and permittivity was reported by Van Uitert [34], who also explained it in terms of increased homogenity and structural perfection with the increase in sintering temperature.

4. Conclusion

The x-ray diffraction studies reveal that even samples prepared at low temperature are crystalline and sintering at higher temperature enhances the purity of the sample. Porosity of the samples decreases upon firing and the samples fired at 900 °C attain 95% of the theoretical density. The coercivity increases with the size of the grains, reaches a maximum and then decreases. This is due to the transition from a multidomain to a single domain structure. Magnetization measurements show deviation in saturation magnetization (M_s) values with respect to its bulk counterparts. This variation in the magnetization values is partly attributed to the formation of α-Fe_2O_3 because of the volatization of $Li_{0.5}Fe_{2.5}O_4$. However the large discrepancy in the magnetization value in as-prepared ultra fine samples has been attributed to the contribution from aligned surface spins. The electrical parameters, namely, dielectric permittivity and ac conductivity were evaluated for all the samples and studied as a function of frequency, temperature and size of the particles. The dependence of both dielectric permittivity and the ac conductivity with frequency is in good agreement with Koops phenomenological theory of dielectric dispersion. There exist possibilities of employing $Li_{0.5}Fe_{2.5}O_4$ for various applications including high power microwave devices and memory devices.

Acknowledgments

MG acknowledges UGC for the financial assistance received under the Faculty Improvement Programme, MRA and SSN acknowledge DST (Government of India) for funding (File No- SP/S2/M-64/96). AMJ is thankful to DST for financial assistance in the form of a post-doctoral fellowship.

References

[1] Dorman J L and Fiorani D 1992 *Magnetic Properties of Fine Particles* (Amsterdam: North Holland)
[2] Soffge F and Schmidbauer E 1981 *J. Magn. Magn. Mater.* **24** 54
[3] EI-Hilo M, Chantrell R W and Grady K O 1998 *J. Appl. Phys.* **84** 5114
[4] Berkowitz A E, Kodama R H, Makhlouf S A and Parker F T 1999 *J. Magn. Magn. Mater.* **196** 591
[5] Hrianaca I, Caizer C, Savil S and Popovoci M 2000 *J. Adv. Mater.* **2** 634
[6] Caizer C 2000 *Solid State Commun.* **124** 53
[7] Watanabe A, Yamamura H, Moriyoshi Y and Shirasaki S 1981 *Ferrites: Proc. Int. Conf. (Tokyo, September–October 1981)* ed H Watanabe *et al* (Tokyo: Tokyo Centre for Academic Publications) vol 170
[8] Gill N K and Puri R K 1985 *J. Mater. Sci. Lett.* **4** 396
[9] Reddy P V, Reddy M B, Muley V N and Ramana Y V 1988 *J. Mater. Sci. Lett.* **7** 1243
[10] Saxena N, Kunar B K, Zaidi Z H and Srivastva G P 1991 *Phys Status Solidi* a **127** 231
[11] White G O and Patton C E 1978 *J. Magn. Magn. Mater.* **9** 299
[12] Cullity B D 1972 *Introduction to Magnetic Materials* (Reading, MA: Addison-Wesley)
[13] Morrish A H and Hanida K 1981 *J. Appl. Phys.* **52** 2496
[14] Kodama R H, Berkowitz A E, McNiff E J Jr and Foner S 1996 *Phys. Rev. Lett.* **77** 394
[15] Billas I M L, Chatelain A and de Heer W A 1994 *Science* **265** 1682
[16] Shi J, Gider S, Babcock K and Awschalom D D 1996 *Science* **271** 937
[17] Rosenweig R E 1985 *Ferrohydrodynamics* (Cambridge, MA: MIT Press)
[18] Ridgley D H, Lensoff H and Childress H D 1970 *J. Am. Ceram. Soc.* **53** 304
[19] Mazen S A, Metawe F and Mansour S F 1997 *J. Phys. D: Appl. Phys.* **30** 1799
[20] Reddy P V, Sathyanarayana R and Rao T S 1983 *Phys. Status. Solidi* a **78** 109
[21] Verma A, Goyal T C, Mindiretta R G and Gupta R G 1999 *J. Magn. Magn. Mater.* **192** 271

[22] El Hiti M A 1996 *J. Magn. Magn. Mater.* **164** 187
[23] Abdeen A M 1998 *J. Magn. Magn. Mater.* **185** 199
[24] Anantharaman M R, Jagatheesan S, Malini K A, Sindhu S, Narayanasamy A, Chinnasamy C N, Jacobs J P, Reijne S, Seshan K, Smits R H H and Brongersma H H 1998 *J. Magn. Magn. Mater.* **189** 83
[25] Shenoy S D, Joy P A and Anantharaman M R 2004 *J. Magn. Magn. Mater.* **269** 217
[26] Chinnasamy C N, Narayanasamy A, Ponpandian N, Chattopadhyay K, Shinoda K, Jeyadevan B, Tohji K, Nakatsuka K, Furubayashi T and Nakatani I 2001 *Phys. Rev.* B **63** 184108
[27] Ahamed M A and Elhiti 1995 *J. Physique III* **5** 775
[28] Shaikh A M, Bellard S S and Chougule B K 1999 *J. Magn. Magn. Mater.* **195** 384
[29] Ahamed M A, Elhiti, Nimar E I and Amar M A 1996 *J. Magn. Magn. Mater.* **152** 391
[30] Koops C G 1951 *Phys. Rev.* **83** 121
[31] Wagner K W 1973 *Amer. Phys.* **40** 317
[32] Kingery W D, Bowen H K and Uhlmann D R 1975 *Introduction to Ceramics* (New York: Wiley) p 904
[33] Pals M, Brahma P and Chakravarthy D 1994 *J. Phys. Soc. Japan* **63** 3356
[34] Van Uitert L G 1955 *J. Chem. Phys.* **23** 10 1883